

RESEARCH ARTICLE

10.1029/2018MS001297

Key Points:

- Description of a stochastic modification of a spectral nonorographic gravity wave parameterization in a climate model
- The mean state of the upper stratosphere and mesosphere is modified by a stronger residual meridional circulation with the stochastic scheme
- The properties of the quasi-biennial oscillation change under a stochastic forcing, with a shorter period and reduced variability

Supporting Information:

- Supporting Information S1

Correspondence to:

F. Serva,
federico.serva@artov.isac.cnr.it

Citation:

Serva, F., Cagnazzo, C., Riccio, A., & Manzini, E. (2018). Impact of a stochastic nonorographic gravity wave parameterization on the stratospheric dynamics of a general circulation model. *Journal of Advances in Modeling Earth Systems*, 10, 2147–2162. <https://doi.org/10.1029/2018MS001297>

Received 16 FEB 2018

Accepted 7 AUG 2018

Accepted article online 13 AUG 2018

Published online 4 SEP 2018

©2018. The Authors.

This is an open access article under the terms of the Creative Commons Attribution-NonCommercial-NoDerivs License, which permits use and distribution in any medium, provided the original work is properly cited, the use is non-commercial and no modifications or adaptations are made.

Impact of a Stochastic Nonorographic Gravity Wave Parameterization on the Stratospheric Dynamics of a General Circulation Model

F. Serva^{1,2}, C. Cagnazzo², A. Riccio¹, and E. Manzini³

¹Department of Science and Technology, Parthenope University of Naples, Naples, Italy, ²Institute of Atmospheric Sciences and Climate, National Research Council, Rome, Italy, ³Max Planck Institute for Meteorology, Hamburg, Germany

Abstract The general circulation of the middle atmosphere, particularly of the mesosphere, is strongly dependent on the forcing arising from gravity wave processes. Their sources in the troposphere are both orographic and nonorographic, the latter being strongly intermittent. In climate models, the effects of gravity waves need to be parameterized, often assuming that their properties are constant. In this work we focus on the changes of the middle atmosphere due to the introduction of intermittency in a parameterization of nonorographic gravity waves, using a stochastic version of the Hines scheme. The stochastic approach is tailored to the diagnosed sensitivity of the model to this forcing, and peculiar changes emerge even if a relatively small amount of intermittency is prescribed. We analyze in detail the changes of the stratospheric dynamics in the tropical region and the global circulation of the middle atmosphere, when the stochastic parameterization is employed in place of the deterministic one. The mean state and variability of the model, realistic also in the default version, are preserved when stochasticity is added. Significant changes are observed in the mesosphere due to an enhanced poleward transport, leading to warming in the winter season. While there are some improvements of the mean state, the interannual variability is not significantly affected in the extratropics. The impacts on the simulated equatorial stratosphere are evident, as the stochasticity reduces the overall period of the quasi-biennial oscillation but also leads to a net reduction of the variability between cycles.

Plain Language Summary Present-day climate models are not able to simulate small-scale phenomena, which are represented by means of simplified descriptions. Among these processes, atmospheric gravity waves are important for the upper atmosphere, as they influence its structure, interacting with the mean flow. These small waves are often associated to convection, but their intermittent nature is not always present in climate models. Here we describe how this property can be included in the representation of gravity waves and which are the effects on the simulated upper atmosphere.

1. Introduction

Subgrid scale atmospheric motions, such as those related to orography and transient weather systems, cannot be directly resolved by general circulation models (GCMs) with a horizontal resolution of ~100 km but are nonetheless important for a realistic simulation of the atmosphere. Among these, gravity waves (GWs), which originate from stationary and transient sources, are important for the dynamics of the middle atmosphere (altitudes between 10 and 100 km), as for example for the zonal mean zonal wind reversal at the mesopause (Houghton, 1978). The inclusion of a representation of orographic GWs (OGWs) is necessary for a realistic numerical simulation of the extratropical circulation, as first shown by Palmer et al. (1986). Also, GWs of nonorographic origin (NOGWs) must be represented in order to close the stratospheric jets (Boville, 1984; Pawson et al., 2000) and to force the quasi-biennial oscillation (QBO; Baldwin et al., 2001) in the equatorial stratosphere, a quasi-periodic oscillation between easterly and westerly wind regimes observed between about 100 and 1 hPa. On a global scale, GWs are an important forcing of the summer branch of the Brewer-Dobson circulation (Butchart, 2014) and must therefore be included in models with inadequate resolution in order to simulate the interhemispheric exchanges.

The detailed comparison exercise presented by Geller et al. (2013) highlighted important differences between observations and models in the GW forcing in the middle atmosphere, as both the intensity and the variability

are underestimated in most modern climate models. In such models, the GW forcing has to be parameterized, since the cost of running high-resolution simulations for climate studies remains prohibitive (Kawatani et al., 2011). This bias in representing NOGWs may originate from the formulation of most parameterizations: they rely on a certain number of tuning parameters, often not constrained by observations, and neglect subgrid variance (they are in most cases not coupled to their modeled sources, which in turn can have biases in low and mixed resolution simulations, as discussed by Krismer et al., 2015). In the last decade, many attempts at coupling sources and GWs have been made, often using multiwave rather than globally spectral parameterizations, such as that used here. In the spectral case, the GW spectrum emerging from the troposphere is treated as a whole, and the deposition of momentum to the mean flow is based on nonlinear dissipation mechanisms. In multiwave approaches, the GW spectrum is instead discretized with a number of independent waves, with results comparable to that of spectral schemes (de la Cámara et al., 2014; Garcia et al., 2017; Lott & Guez, 2013; McCormack et al., 2015). Multiwave approaches are appealing for their modest computational cost and also for the possibility to use the linear theory of GWs to adjust the wave characteristics using simulated precipitation and fronts, producing a consistent response to changes in the source properties. Interactive NOGW schemes have been tested with success in different climate models, such as Charron and Manzini (2002), Schirber et al. (2014), Beres et al. (2005), Chun et al. (2008), Lott and Guez (2013), de la Cámara and Lott (2015), de la Cámara et al. (2016), and Bushell et al. (2015), among others. In order to improve model performances and to mimic the observed properties of the wave forcing, multiwave parameterizations in some cases used a stochastic representation of NOGW variables. In general, two approaches can be used to introduce intermittency in the simulated NOGW forcing: linking the spectrum parameters to the modeled source properties or directly prescribing intermittency through stochasticity. Since there are still important uncertainties in the setup of interactive schemes (Schirber et al., 2015), testing the capabilities of a simple stochastic approach is of large interest, given the effort needed to fully couple sources to spectrum parameters.

In the vast majority of the Coupled Model Intercomparison Project—Phase 5 (Taylor et al., 2012) generation of climate models, subgrid phenomena are represented with different types of deterministic parameterizations, taking as input the large-scale variables and computing the impact of the smallest scale motions on a given grid point. As parameterizations are meant to represent the bulk effects of the small on the large scales, the subgrid scale variability is neglected, leading to a source of error in the simulation. A novel paradigm in the treatment of subgrid scales in weather and climate models is that of stochastic parameterizations, which have the potential to reduce the uncertainty of climate prediction and to improve the realism of the simulation (Palmer, 2012). As for the deterministic case, some form of *tuning* is necessary in order to obtain a significant advantage from the introduction of stochasticity, always considering the physical reasons for the choices made: for example, nonlocal approaches are likely to be more appropriate if the modeled phenomena extend outside a model cell (Palmer, 2001). Due to the intermittent nature of the NOGW sources, such as convective processes, their stochastic representation appears to be quite natural. More than a decade ago, Piani et al. (2004) demonstrated that a model can begin generating a QBO when a stochastic Hines parameterization of NOGWs is employed (however, the impact on the extratropics was not discussed). Without altering the structure of the default spectral scheme, applied globally and constant in time, we want to study the effects of stochasticity on the simulation of the middle atmosphere, using a model which is realistic also in its standard version.

2. Methods

2.1. The ERA-Interim Reanalysis

The reference data set in this work is the European Center for Medium-Range Weather Forecasts reanalysis ERA-interim (ERAi; Dee et al., 2011), covering the period 1979 to present (here we use data from 1979 to 2015). The forecast model is the Integrated Forecasting System (IFS), second release of the 31st cycle, with a sequential four dimensional variational analysis assimilation scheme and variational bias adjustment for the assimilated satellite radiances. The atmospheric model resolution is T255L60, with the model top around 0.1 hPa, and the variables are provided on a $1^\circ \times 1^\circ$ regular grid, interpolated from the original hybrid sigma-pressure to isobaric levels. Even if the vertical domain reaches the lower mesosphere, the reliability of the reanalysis in the proximity of the model top may be limited, due to the difficulty of assimilating observations in the region (Kobayashi et al., 2009) and the enhanced diffusion in the sponge layer. The IFS model of ERAi represents the interaction of NOGWs with the mean flow by means of a Rayleigh friction (McLan-dress, 1998) and is not able to internally generate a QBO (Orr, 2009; Orr & Wedi, 2009). However the ERAi

reanalysis presents a realistic QBO largely determined by the assimilation of high-quality radiosonde observations at the equator, which are a strong constraint on the zonal wind in the region (Kawatani et al., 2016).

2.2. Numerical Model and Experimental Design

In this work we present the analyses of two atmosphere-only simulations of the MA-ECHAM5 model (Manzini et al., 2012; Roeckner et al., 2003), which is used in its T63L95 configuration, corresponding to a resolution of $\sim 2^\circ$ or 200 km in the horizontal and of about 700 m in the stratosphere (with a hybrid sigma-pressure coordinate system on a Lorenz grid). The vertical domain reaches 0.01 hPa, where a diffusive sponge layer prevents the spurious reflection of upward propagating waves. The simulations presented here cover the period from January 1960 to December 2009 and are started from the same initial conditions, obtained after 1 year of model spin up. The simulated wave-mean flow interaction in the middle atmosphere is well represented (Giorgetta et al., 2002; Manzini et al., 2012): The effects of GWs are parameterized following Lott and Miller (1997) for the OGWs and Hines (1997a, 1997b) for the NOGWs. The radiation scheme differs from the default of MA-ECHAM5, as here we use the updated version of Cagnazzo et al. (2007), with six bands instead of four in the shortwave range, better suited to represent radiation-ozone interaction. The boundary conditions (BCs) used for the two simulations are those suggested for the Coupled Model Intercomparison Project—Phase 5 initiative (Taylor et al., 2012) and include interannually varying observed sea surface temperatures and sea-ice, while for ozone, sulfate aerosols and greenhouse gases observations are used up to 2005 and the RCP4.5 scenario afterward. These BCs are the same used for the experiment 1 of the QBOi initiative (Hamilton et al., 2015), an intercomparison project aimed at improving the representation of the QBO in GCMs (<http://www.sparc-climate.org/activities/quasi-biennial-oscillation/>, last accessed: January 2018). The two model versions differ only by the NOGW perturbation of the horizontal wind field at the launching level, with a constant value for the experiment named CTL (1 m/s) and a variable value for the sensitivity experiment, named G02, which is detailed in the following.

2.3. Stochastic Source Parameterization

In current GCMs, the effects of GW dissipation on the middle atmosphere need to be parameterized to obtain a realistic climate. The emission of NOGWs is generally assumed to be constant in time and occurring at every grid point, leading to modest spatial and temporal variability. In order to produce consistent latitudinal or seasonal changes in the NOGW forcing, the properties of parameterized waves are in some cases related to the resolved flow characteristics. In the case of multiwave schemes, this goal can be achieved using the linear theory of GWs, while this is less immediate with globally spectral parameterizations. Possibly also for this reason, the forcing obtained with commonly used spectral schemes does not match that inferred from observations (Geller et al., 2013).

With these schemes, it is common to assume fixed values for the NOGW spectrum, even if some parameters cannot be measured and are adjusted as needed. Here we want to study the effects of a simple stochastic modification, applicable to most spectral schemes, that consist in randomly assigning the amplitude of the NOGW forcing at the lowest active level. This is a positive scalar quantity, which is usually tuned depending on the model configuration: given the lack of observational constraints, it is a reasonable candidate for a stochastic description. Some wave parameters, such as the spectral shape or the anisotropy at the lower level, are either better characterized from observations or not common to different schemes. For simplicity, here we only modify the amplitude of the forcing at the launching level, and other parameters are not changed.

The MA-ECHAM5 model represents the NOGWs by means of the Hines Doppler spread parameterization (DSP), based on the Doppler spread theory (DST), which are described in Hines (1997a, 1997b). The aim of the scheme is to represent the deposition of momentum flux from a broad spectrum of GWs, assumed to propagate vertically from the troposphere, where transient sources are located, to upper levels. This is done by neglecting the Coriolis effect (as the DST is developed for the midfrequency GWs; Fritts & Alexander, 2003), without coupling to the sources, with all the parameters fixed and independent for each time step and grid point.

The fundamental characteristic of the DSP is in the expression for the cutoff of the vertical wavenumber spectrum (as waves with larger m are assumed to be obliterated), which for the j th azimuth reads

$$\{m_j\}_{\text{trial}} = N_i(Nm_M^{-1} + V_j - V_{ji} + \Phi_1\sigma_j)^{-1}, \quad (1)$$

where N is the Brunt-Väisälä frequency, Φ_1 is an adjustable parameter, m_M is the maximum wavenumber before instability and dissipation, V_j is the background wind, and σ_j is the NOGW-induced wind variance

(the subscript i indicates values at the launching level). The calculation is repeated at each grid point starting from the lowermost level (around 600 hPa in log-pressure height), where the root mean square NOGW fluctuation (σ_T , in m/s, subscript T for total) is specified and uniformly distributed among $J = 8$ regularly spaced azimuths, that is, $\sigma_{ji} = \sigma_T J^{-1}$. A minimum number of eight azimuths is recommended by Hines (1997a) for allowing directional cross interaction and has been employed in previous studies, for example, Giorgetta et al. (2006). The vertical divergence of the momentum flux is the quantity which leads to acceleration or deceleration of the mean flow, and the occurrence thereof is dependent on the perturbation at the launching level and the background atmospheric conditions.

The stochastic modification of the Hines parameterization we present here is obtained by extracting, at each time step and grid point, a random value for σ_T from a quasi-Gaussian probability density function (PDF) with a standard deviation of 0.2 m/s but with the same mean of the model default version of 1 m/s (note that negative values of the NOGW perturbation are discarded, and σ_T is set to zero in case, and for this reason, the PDF is not strictly Gaussian). With this choice, 95% of the values are between 0.6 and 1.4 m/s, and 68% are between 0.8 and 1.2 m/s. The sensitivity of the model to changes in σ_T has been discussed by Giorgetta et al. (2006), who have shown that when the parameter is increased/reduced by 10%, the QBO period is significantly shorter/longer. This value for the standard deviation of the distribution has been chosen after performing some *stochastic sensitivity* model runs, briefly documented in the supporting information S1. The value of 0.2 m/s for the PDF standard deviation is adopted to have a clear effect from stochasticity and not to degrade the default model climate (the polar vortices are weakened, Figure S1, and the QBO period is too short, Figures S3 and S4, when the PDF is wider).

In the seminal paper of Piani et al. (2004), σ_T values were constrained to follow an exponential distribution, to represent the observed properties of tropical convection. Lognormal distributions have also been found to well describe the observed NOGW momentum fluxes (Geller et al., 2013). In any case, we found that with long-tailed PDFs, both the mean state and variability of the model are severely degraded (e.g., the QBO becoming overly strong and fast, not shown). Therefore, our quasi-Gaussian PDF is here used as a device to introduce intermittency in this model, a key aspect of the NOGW dynamics (de la Cámara et al., 2016), which is missing in the deterministic version. We note that this sensitivity to the PDF width contradicts Williams et al. (2004), who report that for a stochastic Hines scheme the choice of the underlying PDF is unimportant. A possible explanation for this discrepancy is that the properties of the distribution are less relevant when the launching level is close or at the surface level, as substantial filtering would occur already below the stratosphere (Manzini & McFarlane, 1998).

The Hines scheme has been implemented for several atmospheric climate models which extend well above the troposphere, with evident benefits for the simulated climate, compared to more rudimentary NOGW parameterizations (Manzini et al., 1997). In particular, the realism of the simulated QBO (Giorgetta et al., 2002) and that of the extratropical stratosphere in winter (Manzini et al., 2012) is strongly improved. However, some biases are still present, such as the cold-pole problem, described by Butchart et al. (2011), and the excessive regularity of the QBO, discussed by, for example, Anstey et al. (2016).

Notwithstanding the improvements obtained implementing the Hines scheme in climate models, some critical aspects have to be considered. The DST is formulated in a Lagrangian frame, in which the Doppler shift from the background flow is removed from the dispersion relation (Allen & Joseph, 1989), but the added dependence from the background shear due to the Eulerian to Lagrangian transform is not considered (Broutman et al., 2004). The dynamics of the DSP have been studied in detail by Klaassen (2009a, 2009b), who demonstrated that the observed Eulerian tails of the GW spectrum cannot be reproduced following the arguments of the DST. The transform from the Lagrangian to the Eulerian reference frame of the multiwave spectrum is found to be singular, as continuity, adiabaticity, and hydrostasy are violated.

Despite the shortcomings of the DSP, this scheme is still used in several climate models which need to parameterize NOGWs. Moreover, it has been demonstrated by McLandress and Scinocca (2005) that different spectral schemes can be tuned to obtain similar results and that GCMs are not sensitive to the nonlinear dissipation mechanisms adopted. This possibly makes our approach of broader applicability to other globally spectral schemes, even if the verification of this fact is beyond our present scope.

2.4. Quantification of the Wave-Mean Flow Interaction

The interaction of waves with the mean flow determines the thermal and dynamical state of the atmosphere, especially in the stratosphere and above. These processes can be conveniently described using the transformed Eulerian mean (TEM) formalism (Andrews et al., 1987), in which the expression for the time evolution of the zonal mean zonal wind is given by

$$\partial_t \bar{u} = \partial_t \bar{u}|_{\nabla, \mathbf{F}} + \partial_t \bar{u}|_{adv} + \bar{X}, \quad (2)$$

where

$$\partial_t \bar{u}|_{\nabla, \mathbf{F}} = [a \cos(\phi) \rho_0]^{-1} \nabla \cdot \mathbf{F}, \quad (3)$$

$$\partial_t \bar{u}|_{adv} = -(\bar{v}^*, \bar{w}^*) \{ (a \cos(\phi))^{-1} \partial_\phi [(\cos(\phi) \bar{u}) - f], \partial_p \bar{u} \}. \quad (4)$$

The residual meridional and vertical velocities defined as $\bar{v}^* = \bar{v} - \partial_p(\overline{v'\theta'}/\partial_p\bar{\theta})$, $\bar{w}^* = \bar{w} + (a \cos(\phi))^{-1} \partial_\phi(\overline{v'\theta'} \cos(\phi)/\partial_p\bar{\theta})$, \bar{X} indicates small-scale forcing, $\mathbf{F} = a \cos(\phi)(\partial_p(\overline{u'v'\theta'}/\partial_p\bar{\theta}) - \overline{u'v'})$, $[f - (a \cos(\phi))^{-1} \partial_\phi(\bar{u} \cos(\phi)) \overline{v'\theta'}/\partial_p\bar{\theta} - \overline{u'\omega'}]$ is the Eliassen-Palm flux. In previous equations, ∂_d is the partial derivative with respect to d , a is the Earth radius, f the Coriolis parameter, ϕ is latitude, zonal means and anomalies are indicated with a bar and a prime, respectively (for the notation, see Andrews et al., 1987). The TEM quantities are calculated diagnostically for MA-ECHAM5 and ERAi using the 6-hr data, on model and $1^\circ \times 1^\circ$ grid, respectively, on pressure levels as close as possible to model levels. The mass residual stream function (in units kg/s), driven by the interaction between waves and the mean flow, can be used to describe the interhemispheric circulation (Butchart, 2014) and is defined as

$$\bar{\chi}^*(p) = \frac{2\pi a \cos(\phi)}{g_0} \left(\int_p^{p_{top}} \bar{v} dp - \frac{\overline{v'\theta'}}{\partial_p\bar{\theta}} \right), \quad (5)$$

where g_0 is a reference constant gravitational acceleration.

3. Results and Discussion

3.1. The Zonal Mean Circulation

The zonal mean climate for the boreal winter of the reanalysis and the control model is shown in Figure 1. We can see that the mean thermal structure of ERAi is well reproduced by the control model version, but there are some differences: the simulated tropical lower stratosphere is colder than the reanalysis and latitudinal changes are more marked (Figure 1c), while the interannual variability throughout the northern polar middle atmosphere is suppressed (from 9 to 5 K).

Compared against the CTL version, the boreal middle atmosphere of the stochastic version (Figure 2a) is warmer (around 1.5 K), while the austral is colder: this fact could be caused by a more sustained meridional circulation in the mesosphere using the stochastic parameterization. Similar conclusions are reached when the TEM framework is considered, as discussed below. The winter mesosphere of the stochastic model is generally more variable compared to the deterministic version (Figure 2c).

Regarding the zonal mean zonal wind, the mean structure of the CTL model (Figure 1d) is realistic; even if the boreal tropospheric jet is weaker, the core of both the summer and winter stratospheric jets is somewhat stronger than observations, and the polar night jet extends toward the tropical mesosphere (the easterly-westerly transition at tropical latitudes is smoother in ERAi). The interannual variability of the winter stratosphere appears to be underestimated in CTL compared with ERAi (from 10 to 8 m/s), while the QBO signal in the tropics is stronger and is seen over a larger depth, up to 1 hPa. We note however that few in situ observations are assimilated by ERAi above 30 hPa, as sondes are needed to pass the very cold tropical tropopause (Hamilton et al., 2004). As the reanalysis is based mostly on the forecast model at these altitudes, the results for ERAi are less reliable. The difference in the zonal mean zonal wind between G02 and CTL (Figure 2b) suggests that the stochastic modification acts to reduce—by thermal wind balance—the intensity of jets in the upper stratosphere in both hemispheres (also in the summer hemisphere, where planetary waves cannot propagate), with a net westerly difference in the tropical mesosphere around 0.5 hPa, around the semiannual oscillation (SAO) altitudes (Baldwin et al., 2001). The interannual variability of the two model versions (Figure 2d) is similar, differing significantly in the tropical mesosphere and the polar regions, with G02 more variable in the winter hemisphere.

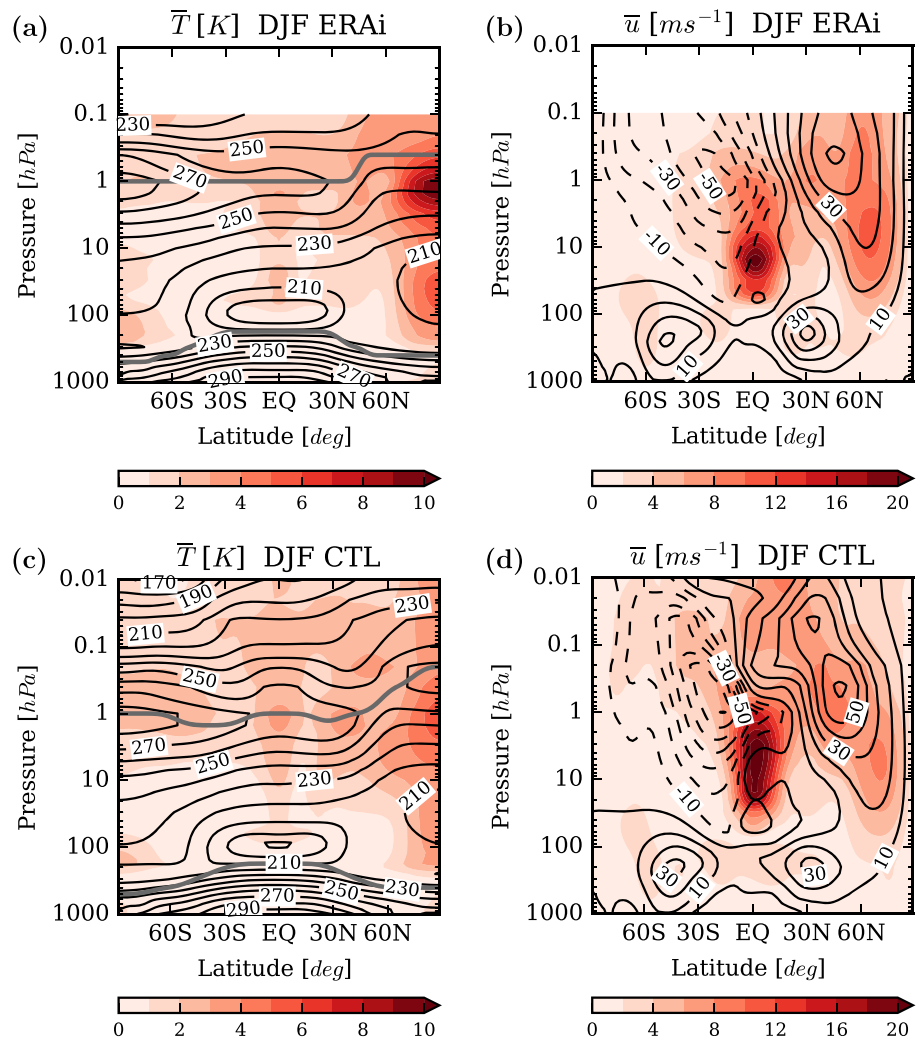


Figure 1. Latitude-height plots of the DJF zonal mean temperature and zonal wind for (a and b) ERA-Interim and (c and d) the CTL model. The mean fields are contoured with black lines; their interannual standard deviations are shaded with colors. The approximate heights of the tropopause and stratopause are indicated with thick gray lines in (a) and (c). DJF = December-January-February.

In order to examine changes at stratospheric levels, we show mean and variability of the zonal mean temperature at 10 hPa in Figure 3. The signature of the annual cycle (and the associated year-to-year variability, larger in the late winter seasons) in ERAi is strong from 30° poleward, while the equatorial region is less variable. The CTL model has a cold bias at the poles in the late winter of both hemispheres and is concurrently less variable, especially in the southern polar region: this cold-pole bias is a common issue with modern climate models and is typically more severe when ozone chemistry is interactive (see, e.g., Butchart et al., 2011). The variability of the default model version is significantly larger than ERAi in the northern extratropics during the boreal spring-summer, when easterlies are established.

While the equatorial region is not different in G02 from CTL (Figure 3, bottom), the stochastic model is warmer during the whole extratropical winter seasons, partly offsetting the model bias, while the variability is not significantly changed between the two versions. Similar significant differences are also found at higher levels (not shown).

As also seen from Figure S1, the changes induced in the extratropical circulation can be substantial when σ_T is made stochastic, such that the stratospheric jet weakening is proportional to the width of the PDF. The profiles for the tendencies computed by the Hines scheme with different σ_T in a winter extratropical case are shown in Figure S2. While the altitudes of the maximum drag are seen to lower as σ_T is increased, the

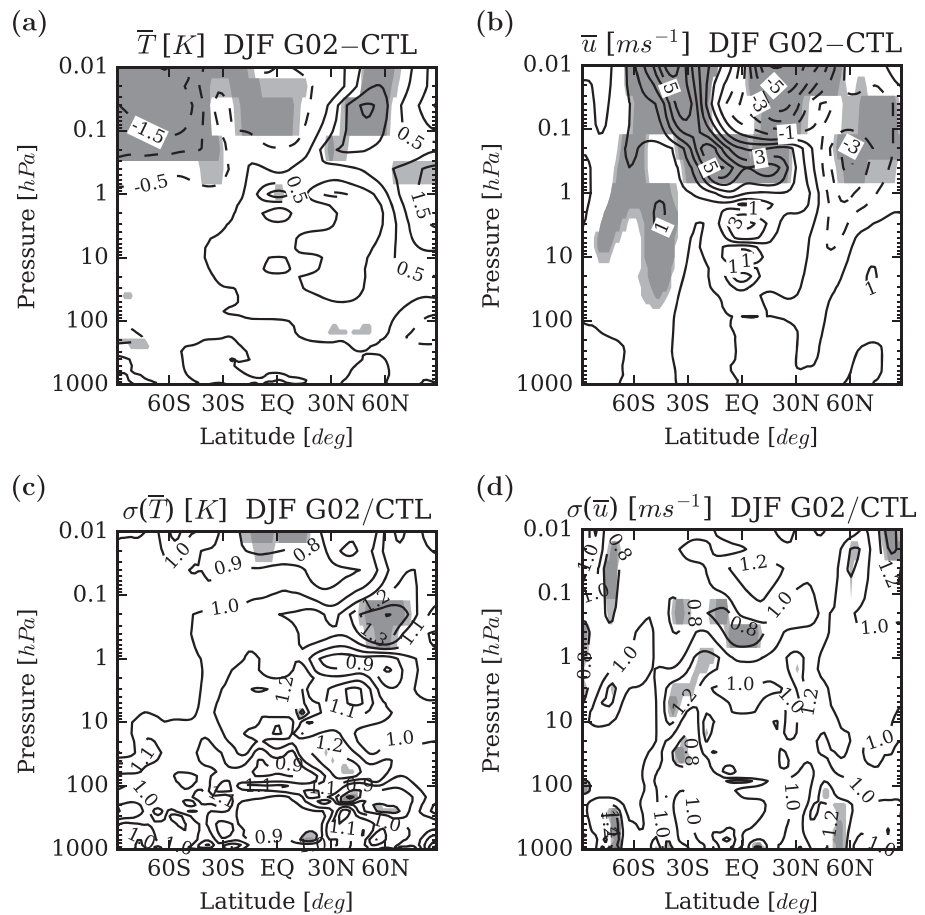


Figure 2. Latitude-height plots of the difference between the mean DJF zonal mean temperature and zonal wind (a and b) and the ratio of the standard deviations for CTL and G02 (c and d). Significances at the 10% and 5% levels (light and dark shadings, respectively) are assessed with a *t* test (a and b) and a *F* test (c and d). DJF = December-January-February.

magnitude of the deceleration varies more dramatically, as it is doubled when the magnitude of the launching level perturbation is larger by 20%. Even if such large decelerations are episodic, their integrated effects are important also for much longer time scales.

A complementary view of the effects induced by the stochastic Hines parameterization on the middle atmosphere is obtained by considering the mean residual circulation, shown in Figure 4 for the boreal winter.

In the Northern Hemisphere, the deep branch of the meridional circulation subsides poleward of 60° N, explaining the warm temperatures characteristic of the winter mesosphere. In the case of ERAi (Figure 4a), as already observed for the zonal mean zonal wind, latitudinal variations of the stream function are smoother than for the models, and the vertical extent of the mesospheric branch is reduced. But we remark that, given the sparse observations assimilated in the lower mesosphere, the reanalysis results are questionable at these altitudes. From Figure 4d, despite the differences between the deterministic and stochastic model versions are relatively small (some percents), a significant tendency for a stronger northward transport in the tropical mesosphere for the stochastic model is observed, consistent with a more sustained NOGW forcing at upper levels, driving the upper branch of the residual circulation. These results are in agreement with the changes in the zonal mean temperature and zonal wind (Figures 2b and 3c), and similar conclusions hold for the austral summer (not shown).

3.2. The Equatorial Stratosphere

The response to a zonal force at the equator is different from that in the extratropics due to the smallness of the Coriolis parameter: at midlatitudes, the steady state circulation resulting from persistent NOGW drag results from a balance between the applied zonal drag and the Coriolis force from a forced meridional circulation (Haynes, 1998). As the effects of the Earth rotation are less important, the main patterns of variability in the

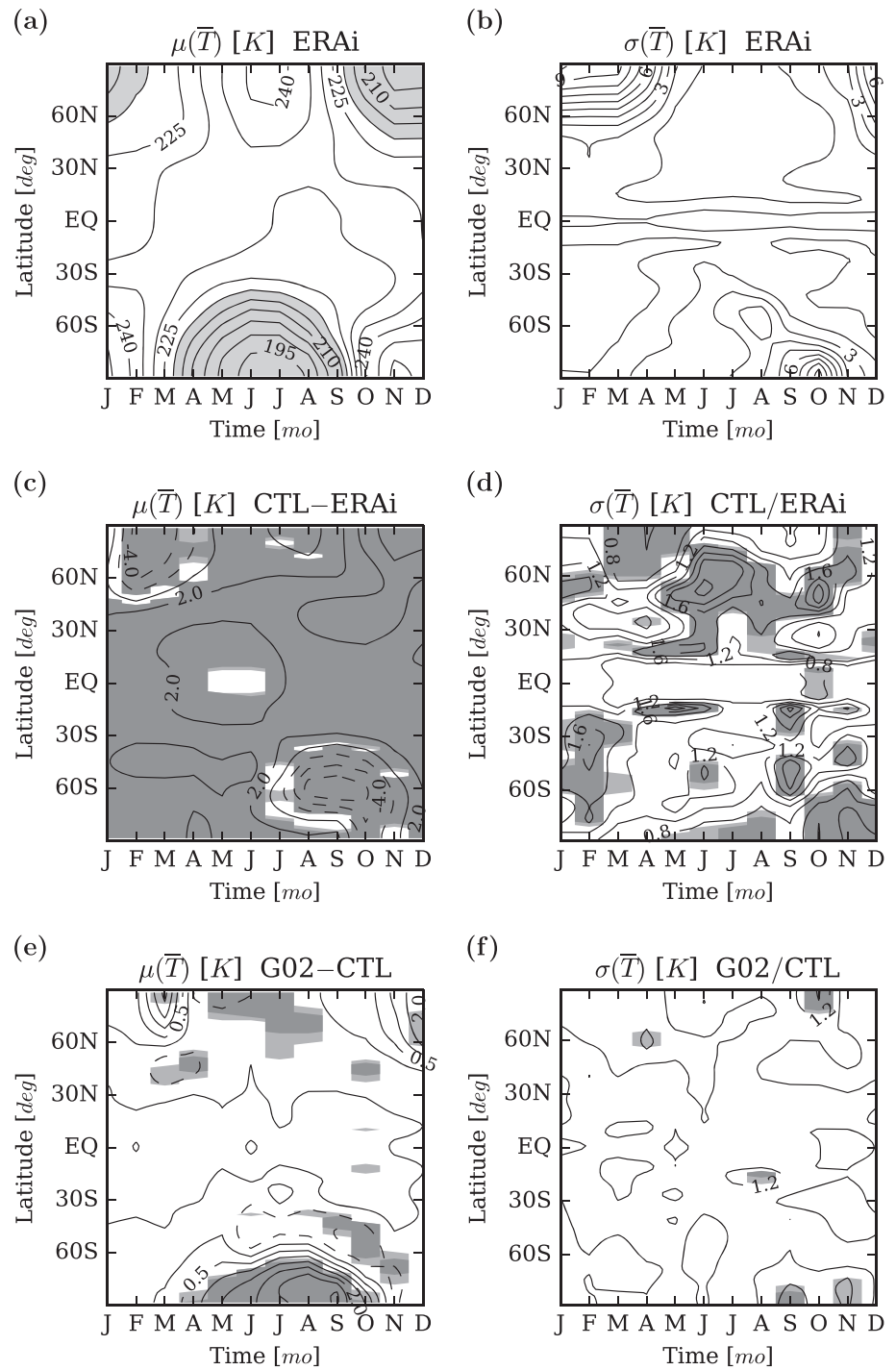


Figure 3. The zonal mean temperature at 10 hPa as a function of the month of the year and latitude. The mean (shadings below 220 K) and interannual standard deviation of ERA-Interim (a and b), the difference of the means and ratio of standard deviations between CTL and ERA-Interim (c and d), and the same for G02 and CTL (e and f). Significances at the 10% and 5% levels (light and dark shadings, respectively) from a *t* test (c and d) and a *F* test (e and f).

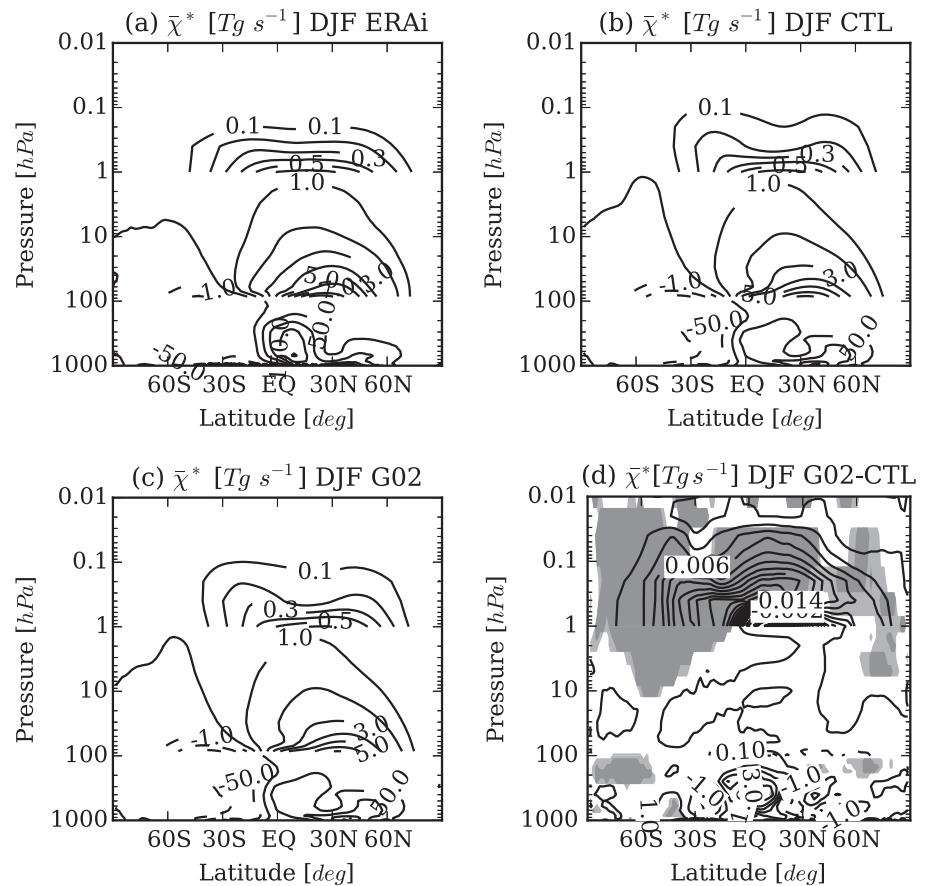


Figure 4. Latitude-height plots of the residual stream function in DJF, for (a) ERA-Interim, (b) the CTL model, (c) the G02 model, and (d) the difference G02 minus CTL. The contour intervals span different orders of magnitude in the troposphere, stratosphere, and mesosphere, with negative contours dashed. Significant differences at the 10% and 5% levels from a *t* test are shaded (light and dark gray, respectively) in (d). DJF = December-January-February.

tropical upper atmosphere are oscillatory and are the QBO in the stratosphere and the SAO in the mesosphere. The forcing of these oscillations comes from waves with different properties excited in the troposphere, such as Kelvin waves, inertio-GWs, and small-scale GWs (Baldwin et al., 2001). GWs likely have the same importance of resolved waves in the momentum balance, but the partitioning between different forcings is not fully understood (Dunkerton, 1997; Ern et al., 2014; Giorgetta et al., 2002).

The representation of the equatorial stratosphere remains a challenge for modern reanalysis systems, as observations are generally sparse both in space and time (Kawatani et al., 2016): for the zonal mean zonal wind, the high-quality radiosonde observations, performed since the 1950s (Naujokat, 1986), pose a strong constrain on the representation of the QBO, at least below 10 hPa. In some cases, the forecast models of reanalyses (like the IFS version of ERAi) are not able to internally generate a QBO (due to a too coarse vertical resolution and an insufficient GW forcing), and therefore, observations are crucial. On the contrary, the MA-ECHAM5 model is capable to simulate a realistic QBO, with the properties of the oscillation sensitive to the parameterized NOGW forcing (Giorgetta et al., 2006).

After the subtraction of the seasonal cycle of the zonal mean zonal wind, the predominance of a biennial variability in the equatorial stratosphere is evident, as shown in Figure 5 for ERAi, the CTL and G02 model versions.

Even if both model versions present a realistic pattern of easterly and westerly bands propagating downward to the lower stratosphere, some differences among them can be noted. It is important to remark that the imposition of stochasticity does not drastically degrade the stratospheric variability at the equator in G02 compared to CTL, as we discuss below. For ERAi (Figure 5a), the westerly shear zones descend more rapidly

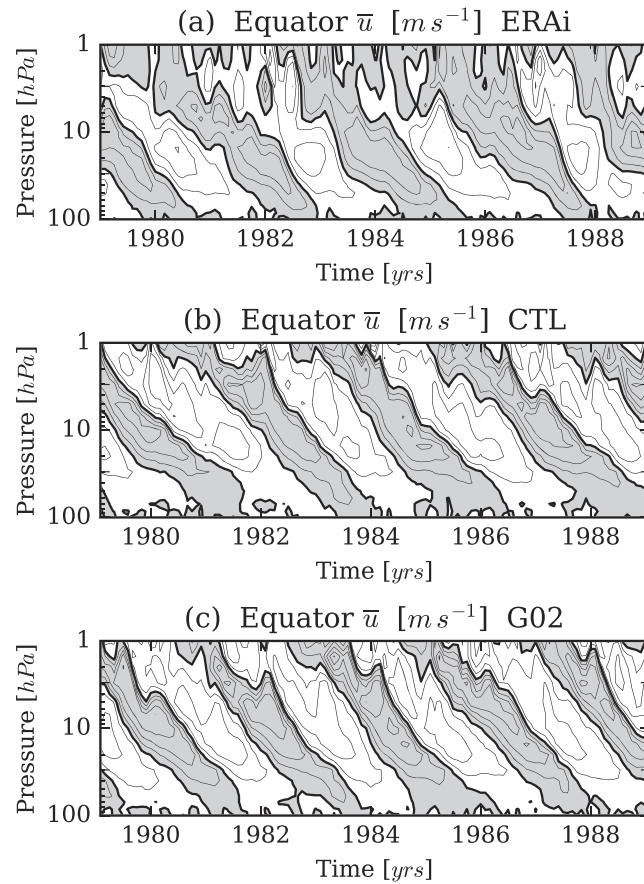


Figure 5. Time-height plots of the deseasonalized zonal mean zonal wind at the equator, for (a) ERA-Interim, (b) the CTL, and (c) the G02 models. Easterlies are shaded, contours every 10 m s^{-1} .

and regularly than their easterly counterpart; in the case of CTL (Figure 5b), the asymmetry between the two phases is less marked, and easterly phases appear to be shorter than the westerly ones; the same can be said for the G02 model (Figure 5c), for which the QBO has a shorter period than CTL. Note how the QBO is less regular in the reanalysis than in the models above 10 hPa, where the assimilation of observations is scarce.

Regarding the QBO period, the Fourier spectrum of the tropical zonal mean zonal wind of ERAi peaks just below 28 months at 20 hPa (Figure 6a), while that of CTL (Figure 6b) is maximized at 30 months and between 20 and 5 hPa and that of G02 (Figure 6c) has a narrow peak just after 26 months, between 20 and 3 hPa.

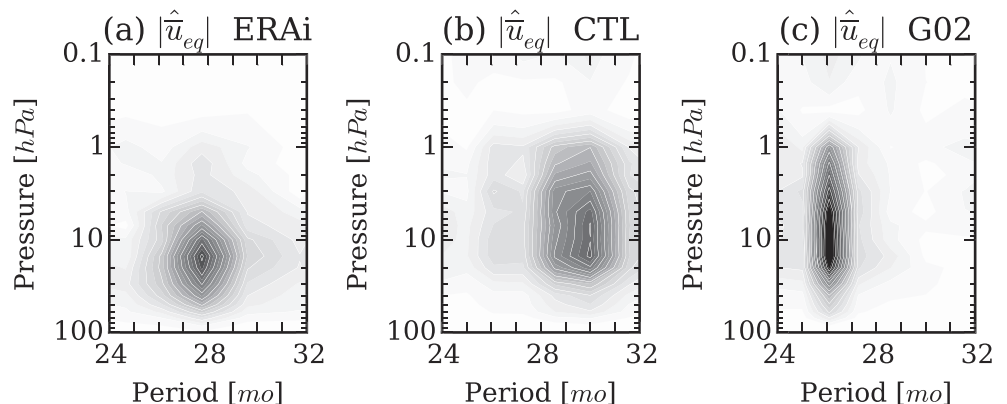


Figure 6. Amplitude of the Fourier spectrum of the deseasonalized zonal mean zonal wind at the equator for (a) ERA-Interim, (b) the CTL, and (c) the G02 models.

Some interesting features to be noted are the simultaneous reduction of the QBO period from CTL to G02 and the much narrower peak around 26 months of G02. As seen in the experiments done varying the spread of the σ_T PDF, described in the supporting information S1, the period of the QBO is inversely proportional to the spread at launching level (Figure S3). It is shown by Giorgetta et al. (2006) that the period is proportional to the mean perturbation at the launching level. Here we see that the response to episodic strong accelerations or decelerations is a faster propagation of the phase: this effect is phase dependent, with the descent of the easterlies more sensitive to changes in σ_T (see Figure S5 and the differences in the jets in Figure S3) than the westerlies. A 20% increase of the launching level perturbation leads to a deceleration at 30 hPa which is a factor two larger than that of CTL (the magnitude is much smaller compared to Figure S2), and the height of the drag maximum is unchanged.

The spread reduction of the QBO period is observed also for other standard deviations of the σ_T PDF (see Figure S4) with the stochastic approach; hence, it does not depend on the exact amount of wavefield variability.

To appreciate the effects of stochasticity on the QBO phase progression, the evolution of both phases at 50 hPa are displayed in Figure 7. The vertical and horizontal red segments indicate the mean and the 2σ interval for the peak values and the duration of each phase, respectively. From the results of ERAi, the asymmetry between the two phases can be noted. The easterly peak is more variable and deeper than the westerly, and the duration of the easterlies is shorter than that of the westerly regime. The two QBO phases in both model versions are more symmetric than in the reanalysis, in particular the peak values of the easterly phase are underestimated. While the asymmetry in the amplitude is marginally larger in G02, the variability of the period is reduced, with the CTL model less regular and comparable to ERAi. These results can be explained in light of the long periodicity of the QBO and Figure S5. Even if the PDF of σ_T is quasi-Gaussian at the launching level, the response of the Hines scheme is nonlinear, and the drag distribution in the stratosphere is skewed toward extreme values. For this reason, the downward propagation of the QBO in G02 is faster regardless of its phase and the variability of the resolved forcing.

To further investigate changes in the simulated dynamics of the QBO, the composites of the vertical zonal mean zonal wind profiles and the Hines tendencies, for the easterly onset at the 20-hPa level are shown in Figure 8. As previously noted, the modeled depth of the QBO is larger in the CTL model compared to the reanalysis, and this is evident also during the onset. In the CTL simulation (Figure 8b), the forcing from NOGWs is larger between 10 and 1 hPa, and in this phase the acceleration calculated from the Hines parameterization reaches the largest absolute values. The differences between the two model versions are made clear considering Figure 8c, showing the zonal mean zonal wind and Hines tendency, always at 20 hPa. While the amplitude of the QBO is unaltered going from the CTL to the G02 model version, the period of the latter is clearly shorter, and the same holds for the tendency from NOGWs, which is also slightly larger (within $5 \text{ cm} \cdot \text{s}^{-1} \cdot \text{day}^{-1}$) just after the onset and around month 13 and 28 afterward. Summarizing, for both models, the QBO extends over a larger depth compared to ERAi, and the tendency from NOGWs, larger during the westerly to easterly transition, leads to a faster downward phase propagation in the stochastic model version; the main differences between CTL and G02 are the shorter periodicity of the QBO and larger values for the tendencies computed by the Hines parameterization.

The downward propagation of the QBO has phase-specific features, which can be observed in the profiles of the zonal mean zonal wind, resolved and parameterized tendencies composited at the onsets (Figure 9). During the westerly onset, the acceleration is larger at 20 hPa, stronger in G02 than in CTL (40 and $20 \text{ cm} \cdot \text{s}^{-1} \cdot \text{day}^{-1}$). The resolved and parameterized wave forcings have the same sign, and their magnitude is the same. At upper levels, the absolute values of the opposing advection and parameterized wave forcing are reduced in G02 compared to CTL, and the net tendency in the stochastic model is more negative. At the easterly onset, the G02 model presents two distinct peaks in the net tendency: an easterly peak just above 20 hPa (dominated by the NOGW contribution, around $-35 \text{ cm} \cdot \text{s}^{-1} \cdot \text{day}^{-1}$, and resolved waves, around $-20 \text{ cm} \cdot \text{s}^{-1} \cdot \text{day}^{-1}$), and a westerly maximum around 5 hPa (mainly from resolved waves, around $20 \text{ cm} \cdot \text{s}^{-1} \cdot \text{day}^{-1}$, less from NOGWs). While the peak at the lower level is stronger than in CTL due to NOGWs, the main difference in the higher peak is caused by advection. The role of intermittent and strong tendencies provided by the stochastic Hines scheme appears more clearly around 20 hPa, with stronger accelerations in G02. However, the relative role of resolved and parameterized tendencies does not change qualitatively between the two model versions, since the resolved dynamics of the QBO are not directly affected by the stochastic scheme. The robustness of

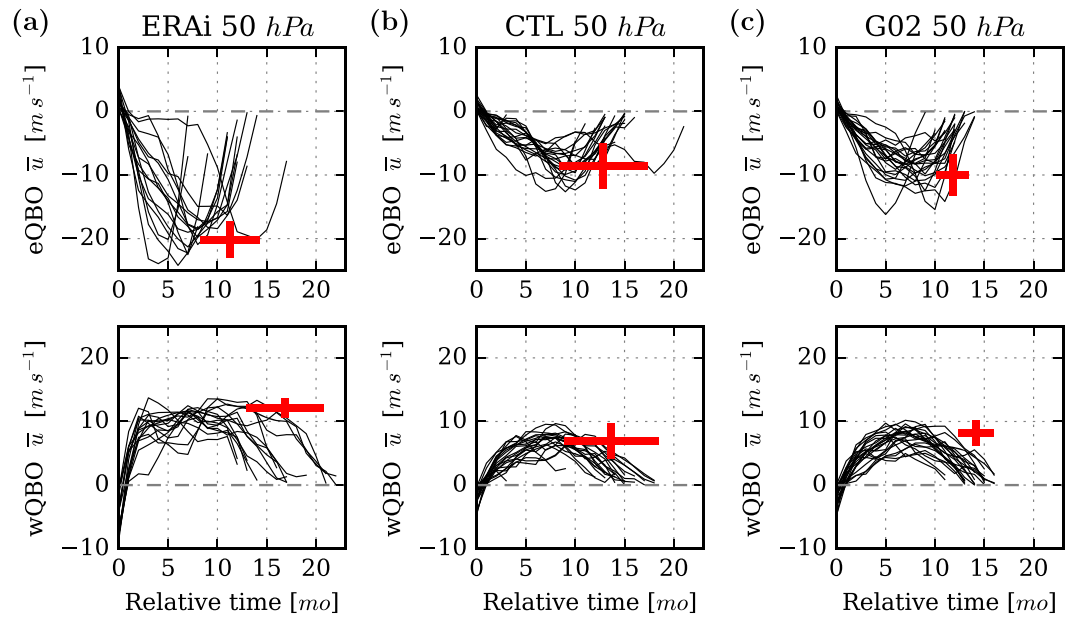


Figure 7. The zonal mean zonal wind (black lines) at the equator following the onset at 50 hPa, for both phases. The horizontal and vertical red lines indicate the mean and the 2σ interval for the periods and peak values, respectively. Plots for ERA-Interim (a), the CTL (b), and G02 (c) model versions. QBO = quasi-biennial oscillation.

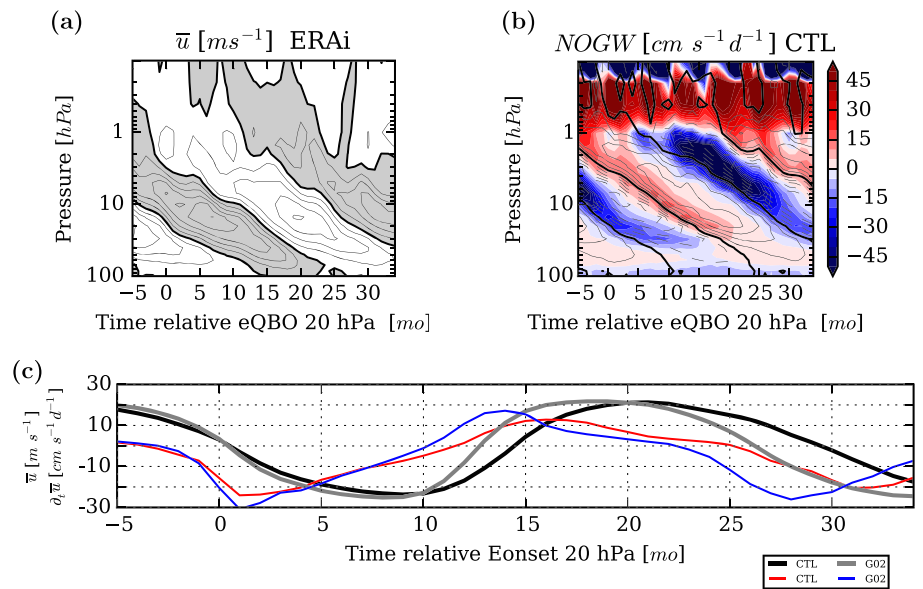


Figure 8. Time-height plots of the equatorial zonal mean zonal wind for ERAi and CTL, deseasonalized and composited at the easterly onset at 20 hPa (a and b; tendency from the Hines scheme is shaded in b). Time series of the same fields (thick lines for the zonal wind, thin for the tendencies) at 20 hPa for the CTL and the G02 model versions (c). NOGW = nonorographic gravity waves; ERAi = ERA-Interim; QBO = quasi-biennial oscillation.

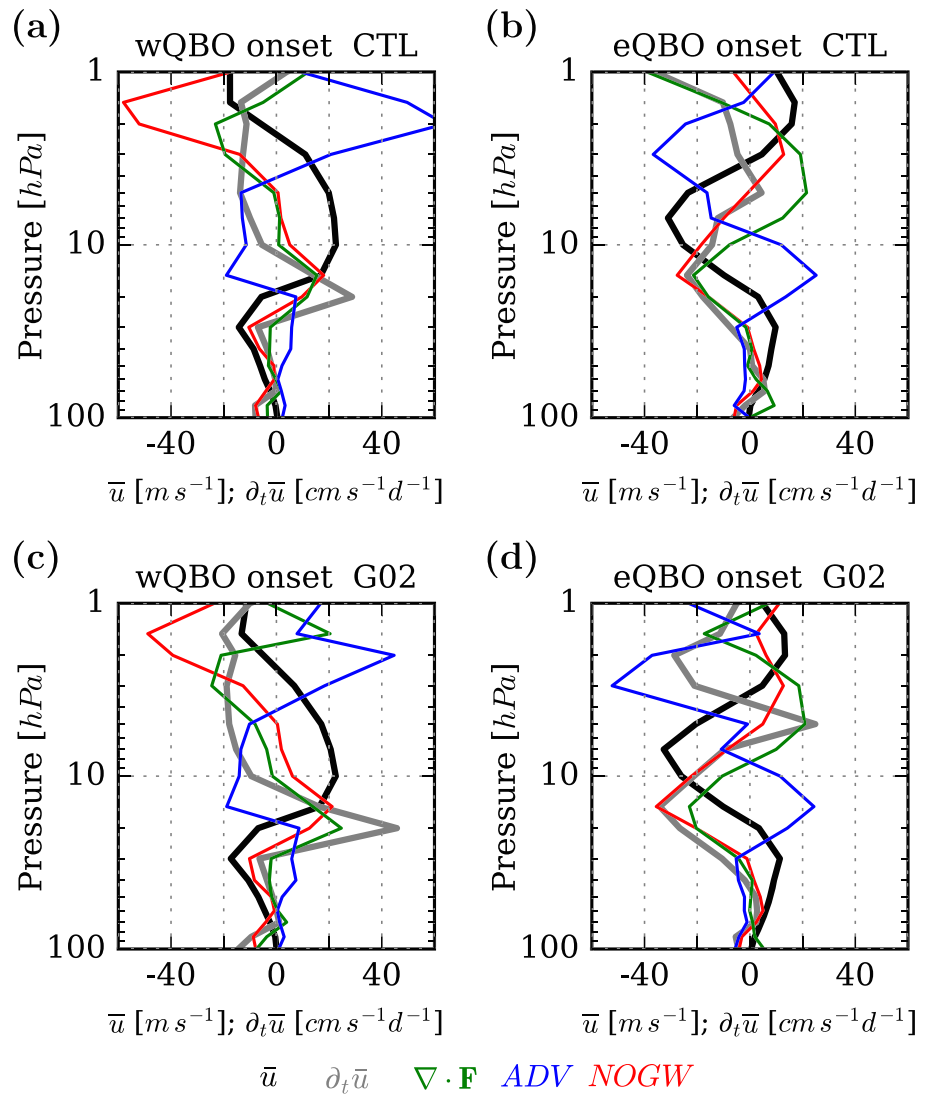


Figure 9. Vertical profiles of the zonal mean zonal wind (thick, black line) and zonal mean tendencies (thick, gray line for net tendency, red line for NOGWs, blue line for advection, and green line for EP flux divergence) composited at the easterly and westerly onsets at 20 hPa, for the CTL and the G02 models. NOGW = nonorographic gravity waves; QBO = quasi-biennial oscillation.

the resolved forcing makes the properties of the QBO less sensitive to specific changes of the parameterized wave driving in this model.

4. Conclusions

In this work we discuss the impacts on the simulation of the stratospheric dynamics of a stochastic modification of the NOGW parameterization of Hines, already implemented in the MA-ECHAM5 model. We compare the simulation of the recent past performed with a control and a stochastic model version, using the ERAi reanalysis as a reference.

The relevance of randomness for weather and climate simulation is currently debated, as stochastic techniques have been found to alleviate some of the shortcomings deriving from the traditional *resolved* and *unresolved* scales approach. Stochastic techniques in climate modeling have been used with success to increase the spread in ensemble simulations and also to increase the variability of the subgrid scales of the simulation. A probabilistic representation of NOGWs appears to be justified, since while their sources in the atmosphere are highly intermittent (e.g., convection), this variability is generally not included in GCM

parameterizations, which are often lacking strong observational constraints. Moreover, there are large uncertainties whether the *static* formulations, often calibrated for the present conditions, are adequate for representing different climates.

Without changing other aspects of the Hines scheme, we extracted random values of the horizontal wind perturbation from NOGWs from a quasi-Gaussian PDF: the details of the distribution are chosen to preserve the realistic mean state of the default model but also to add a notable stochastic component to the simulation. The imposition of stochasticity does not change the dynamics of the Hines scheme but leads to episodic large differences in the magnitude of the computed tendencies, and to a lower degree, to changes in the levels where the drag on the mean flow is applied. But as shown in the supporting information S1, allowing for a too large variability of the wavefield at the launching level is detrimental to the model results. It is interesting to note that, by constraining the global NOGW forcing at the launching level to a simple PDF (chosen on empirical basis), it is possible to ameliorate some of the model biases, preserving the realistic aspects of the simulation, without ad hoc spatial or temporal modulations.

The effects of the stochastic modification are evident in the solstice mesosphere of the extratropics, with the net effect of slowing the polar night jet and warming at the upper levels, also due to a strengthening of the mean residual circulation from the summer to the winter hemisphere. The realism of the deterministic version is preserved also using the stochastic scheme, and the bias at high latitudes is reduced. While the extratropical mean state is significantly improved, the interannual variability is underestimated also in the stochastic version.

GWs are ubiquitous in the middle atmosphere at the equator, where convective systems are more frequent, and they represent an important contribution to the momentum balance in the region. The deterministic model version, with a fine vertical resolution and the Hines parameterization, internally generates realistic QBO and SAO, both sensitive to changes in the NOGW forcing. The result obtained with the stochastic parameterization is to force a QBO with a similar amplitude, but the descent is more regular and faster, with a reduced period somewhat closer to that of the reanalysis. The relative importance of resolved and parameterized contributions to the momentum balance is similar in the two model versions and depends on the phase of the QBO. However, the intercycle variability is further reduced, possibly as a result of the episodic strong accelerations produced within the stochastic scheme (discussed in supporting information S1). For this reason, other strategies should be followed to improve the simulated QBO variability on long time scales.

Both observational and modeling studies demonstrated that intermittency is a key feature of NOGW dynamics, which should be included in GCMs. This can be achieved by linking the properties of parameterized NOGWs to the characteristic of the resolved flow or by directly adding stochasticity to the model. The link between sources and NOGW properties, as their relationship is not well understood, is necessarily done on empirical basis (Schirber et al., 2015). And while linking with the sources leads to spatial and temporal variability and to increased drag in the lower stratosphere (Bushell et al., 2015; de la Cámara et al., 2016), the dynamical filtering by the background winds reduces the signature of the sources on the forcing at upper levels. As shown in this work, directly building stochasticity into traditional spectral schemes can be a strategy for improving the simulation of the middle atmosphere under current conditions, particularly for those models with a cold bias in the upper stratosphere or a weak QBO. Compared to interactive NOGW schemes, adding stochasticity would not introduce, by itself, seasonal or long-term variability in the middle atmospheric forcing, possibly a secondary aspect in different climates (de la Cámara et al., 2016). In general, even when the model resolution is largely increased, the parameterized NOGW drag remains a key term of the stratospheric momentum budget (Polichtchouk et al., 2018), and therefore, stochastic NOGW schemes can find application in this case as well.

Given the simplicity of the approach we describe, this could easily be tested using a different setup. It is often the case that the tuning of a model is not robust across different configurations: the same consideration holds for the QBO, which depends on the model resolution, BCs, and parameterized processes. As an example, the simulated QBO in CMCC-CMS, a coupled model based on MA-ECHAM5, is not stable, disappearing entirely at times (see, e.g., Schenzinger et al., 2017, their Figure 1). If applied to an atmosphere-ocean coupled model, it would certainly be interesting to determine whether the calibration of parameters, needed to bring the model climate toward observations, could be relaxed adding stochasticity into the NOGW forcing. And given the criticism that the Hines parameterization has attracted, it would also be important to verify the consistency of the response using other parameterizations, based on different nonlinear dissipation mechanisms.

Acknowledgments

We thank three anonymous reviewers for valuable comments on the manuscript. The comments of the first anonymous reviewer greatly helped improve the discussion on the NOGW schemes and on the issues of the DSP. We acknowledge the ECMWF for the use of their computing facilities under the Special Project SPITCHCG, and for providing the ERA-Interim reanalysis data set. We thank M. Giorgetta and F. Bunzel for the software for the TEM calculations and S. Rast for technical assistance. F. S. has been supported by the European Commission, under grant StratoClim-603557-FP7-ENV.2013.6.1-2. A part of this work was performed while F. S. was visiting at the Max Planck Institute for Meteorology. The ERA-Interim data can be accessed following this link: <http://apps.ecmwf.int/datasets/>, and the model simulation data can be retrieved here: <https://file.sic.rm.cnr.it/index.php/s/kq9tx600EHVesdg>.

References

Allen, K. R., & Joseph, R. I. (1989). A canonical statistical theory of oceanic internal waves. *Journal of Fluid Mechanics*, *204*, 185–228. <https://doi.org/10.1017/S0022112089001722>

Andrews, D. G., Holton, J. R., & Leovy, C. B. (1987). *Middle atmosphere dynamics* (Vol. 40). Orlando, San Diego: Academic press.

Anstey, J. A., Scinocca, J. F., & Keller, M. (2016). Simulating the QBO in an atmospheric general circulation model: Sensitivity to resolved and parameterized forcing. *Journal of the Atmospheric Sciences*, *73*(4), 1649–1665. <https://doi.org/10.1175/JAS-D-15-0099.1>

Baldwin, M. P., Gray, L. J., Dunkerton, T. J., Hamilton, K., Haynes, P. H., Randel, W. J., et al. (2001). The quasi-biennial oscillation. *Reviews of Geophysics*, *39*(2), 179–229. <https://doi.org/10.1029/1999RG000073>

Beres, J. H., Garcia, R. R., Boville, B. A., & Sassi, F. (2005). Implementation of a gravity wave source spectrum parameterization dependent on the properties of convection in the Whole Atmosphere Community Climate Model (WACCM). *Journal of Geophysical Research*, *110*, D10108. <https://doi.org/10.1029/2004JD005504>

Boville, B. A. (1984). The influence of the polar night jet on the tropospheric circulation in a GCM. *Journal of the Atmospheric Sciences*, *41*(7), 1132–1142. [https://doi.org/10.1175/1520-0469\(1984\)041<1132:TOTPN>2.0.CO;2](https://doi.org/10.1175/1520-0469(1984)041<1132:TOTPN>2.0.CO;2)

Brounman, D., Grimshaw, R. H. J., & Eckermann, S. D. (2004). Internal waves in a Lagrangian reference frame. *Journal of the Atmospheric Sciences*, *61*(11), 1308–1313. [https://doi.org/10.1175/1520-0469\(2004\)061<1308:IWIALR>2.0.CO;2](https://doi.org/10.1175/1520-0469(2004)061<1308:IWIALR>2.0.CO;2)

Bushell, A. C., Butchart, N., Derbyshire, S. H., Jackson, D. R., Shutts, G. J., Vosper, S. B., & Webster, S. (2015). Parameterized gravity wave momentum fluxes from sources related to convection and large-scale precipitation processes in a global atmosphere model. *Journal of the Atmospheric Sciences*, *72*(11), 4349–4371. <https://doi.org/10.1175/JAS-D-15-0022.1>

Butchart, N. (2014). The Brewer-Dobson circulation. *Reviews of Geophysics*, *52*, 157–184. <https://doi.org/10.1002/2013RG000448>

Butchart, N., Charlton-Perez, A. J., Cionni, I., Hardiman, S. C., Haynes, P. H., Krüger, K., et al. (2011). Multimodel climate and variability of the stratosphere. *Journal of Geophysical Research*, *116*, D05102. <https://doi.org/10.1029/2010JD014995>

Cagnazzo, C., Manzini, E., Giorgetta, M. A., Forster, P. M. D. F., & Morcrette, J. J. (2007). Impact of an improved shortwave radiation scheme in the MAECHAM5 general circulation model. *Atmospheric Chemistry and Physics*, *7*(10), 2503–2515. <https://doi.org/10.5194/acp-7-2503-2007>

Charron, M., & Manzini, E. (2002). Gravity waves from fronts: Parameterization and middle atmosphere response in a general circulation model. *Journal of the Atmospheric Sciences*, *59*(5), 923–941. [https://doi.org/10.1175/1520-0469\(2002\)059<0923:GWFFPA>2.0.CO;2](https://doi.org/10.1175/1520-0469(2002)059<0923:GWFFPA>2.0.CO;2)

Chun, H.-Y., Choi, H. J., & Song, I. S. (2008). Effects of nonlinearity on convectively forced internal gravity waves: Application to a gravity wave drag parameterization. *Journal of the Atmospheric Sciences*, *65*(2), 557–575. <https://doi.org/10.1175/2007JAS2255.1>

de la Cámara, A., & Lott, F. (2015). A parameterization of gravity waves emitted by fronts and jets. *Geophysical Research Letters*, *42*, 2071–2078. <https://doi.org/10.1002/2015GL063298>

de la Cámara, A., Lott, F., & Abalos, M. (2016). Climatology of the middle atmosphere in LMDZ: Impact of source-related parameterizations of gravity wave drag. *Journal of Advances in Modeling Earth Systems*, *8*, 1507–1525. <https://doi.org/10.1002/2016MS000753>

de la Cámara, A., Lott, F., & Hertzog, A. (2014). Intermittency in a stochastic parameterization of nonorographic gravity waves. *Journal of Geophysical Research: Atmospheres*, *119*, 11,905–11,919. <https://doi.org/10.1002/2014JD022002>

Dee, D. P., Uppala, S. M., Simmons, A. J., Berrisford, P., Poli, P., Kobayashi, S., et al. (2011). The ERA-interim reanalysis: Configuration and performance of the data assimilation system. *Quarterly Journal of the Royal Meteorological Society*, *137*(656), 553–597. <https://doi.org/10.1002/qj.828>

Dunkerton, T. J. (1997). The role of gravity waves in the quasi-biennial oscillation. *Journal of Geophysical Research*, *102*(D22), 26,053–26,076. <https://doi.org/10.1029/96JD02999>

Ern, M., Ploeger, F., Preusse, P., Gille, J. C., Gray, L. J., Kalisch, S., et al. (2014). Interaction of gravity waves with the QBO: A satellite perspective. *Journal of Geophysical Research: Atmospheres*, *119*, 2329–2355. <https://doi.org/10.1002/2013JD020731>

Fritts, D. C., & Alexander, M. J. (2003). Gravity wave dynamics and effects in the middle atmosphere. *Reviews of Geophysics*, *41*, 1003. <https://doi.org/10.1029/2001RG000106>

García, R. R., Smith, A. K., Kinnison, D. E., de la Cámara, A., & Murphy, D. J. (2017). Modification of the gravity wave parameterization in the Whole Atmosphere Community Climate Model: Motivation and results. *Journal of the Atmospheric Sciences*, *74*(1), 275–291. <https://doi.org/10.1175/JAS-D-16-0104.1>

Geller, M. A., Alexander, M. J., Love, P. T., Bacmeister, J., Ern, M., Hertzog, A., et al. (2013). A comparison between gravity wave momentum fluxes in observations and climate models. *Journal of Climate*, *26*(17), 6383–6405. <https://doi.org/10.1175/JCLI-D-12-00545.1>

Giorgetta, M. A., Manzini, E., & Roeckner, E. (2002). Forcing of the quasi-biennial oscillation from a broad spectrum of atmospheric waves. *Geophysical Research Letters*, *29*(8), 1245. <https://doi.org/10.1029/2002GL014756>

Giorgetta, M. A., Manzini, E., Roeckner, E., Esch, M., & Bengtsson, L. (2006). Climatology and forcing of the quasi-biennial oscillation in the MAECHAM5 model. *Journal of Climate*, *19*(16), 3882–3901. <https://doi.org/10.1175/JCLI3830.1>

Hamilton, K., Hertzog, A., Vial, F., & Stenichkov, G. (2004). Longitudinal variation of the stratospheric quasi-biennial oscillation. *Journal of the Atmospheric Sciences*, *61*(4), 383–402. [https://doi.org/10.1175/1520-0469\(2004\)061<0383:LVOTSQ>2.0.CO;2](https://doi.org/10.1175/1520-0469(2004)061<0383:LVOTSQ>2.0.CO;2)

Hamilton, K., Osprey, S. M., & Butchart, N. (2015). Modeling the stratosphere's "heartbeat". *Eos*, *96*, 8. <https://doi.org/10.1029/2015EO032301>

Haynes, P. H. (1998). The latitudinal structure of the quasi-biennial oscillation. *Quarterly Journal of the Royal Meteorological Society*, *124*(552), 2645–2670. <https://doi.org/10.1002/qj.49712455206>

Hines, C. O. (1997a). Doppler-spread parameterization of gravity-wave momentum deposition in the middle atmosphere. Part 1: Basic formulation. *Journal of Atmospheric and Solar-Terrestrial Physics*, *59*(4), 371–386. [https://doi.org/10.1016/S1364-6826\(96\)00079-X](https://doi.org/10.1016/S1364-6826(96)00079-X)

Hines, C. O. (1997b). Doppler-spread parameterization of gravity-wave momentum deposition in the middle atmosphere. Part 2: Broad and quasi monochromatic spectra, and implementation. *Journal of Atmospheric and Solar-Terrestrial Physics*, *59*(4), 387–400. [https://doi.org/10.1016/S1364-6826\(96\)00080-6](https://doi.org/10.1016/S1364-6826(96)00080-6)

Houghton, J. T. (1978). The stratosphere and mesosphere. *Quarterly Journal of the Royal Meteorological Society*, *104*(439), 1–29. <https://doi.org/10.1002/qj.49710443902>

Kawatani, Y., Hamilton, K., Miyazaki, K., Fujiwara, M., & Anstey, J. A. (2016). Representation of the tropical stratospheric zonal wind in global atmospheric reanalyses. *Atmospheric Chemistry and Physics*, *16*, 6681–6699. <https://doi.org/10.5194/acp-16-6681-2016>

Kawatani, Y., Hamilton, K., & Watanabe, S. (2011). The quasi-biennial oscillation in a double CO₂ climate. *Journal of the Atmospheric Sciences*, *68*(2), 265–283. <https://doi.org/10.1175/2010JAS3623.1>

Klaassen, G. P. (2009a). Testing Lagrangian theories of internal wave spectra. Part I: Varying the amplitude and wavenumbers. *Journal of the Atmospheric Sciences*, *66*(5), 1077–1100. <https://doi.org/10.1175/2008JAS2666.1>

Klaassen, G. P. (2009b). Testing Lagrangian theories of internal wave spectra. Part II: Varying the number of waves. *Journal of the Atmospheric Sciences*, *66*(5), 1101–1125. <https://doi.org/10.1175/2008JAS2667.1>

- Kobayashi, S., Matricardi, M., Dee, D., & Uppala, S. (2009). Toward a consistent reanalysis of the upper stratosphere based on radiance measurements from SSU and AMSU-A. *Quarterly Journal of the Royal Meteorological Society*, *135*(645), 2086–2099. <https://doi.org/10.1002/qj.514>
- Krismer, T. R., Giorgetta, M. A., von Storch, J. S., & Fast, I. (2015). The influence of the spectral truncation on the simulation of waves in the tropical stratosphere. *Journal of the Atmospheric Sciences*, *72*(10), 3819–3828. <https://doi.org/10.1175/JAS-D-14-0240.1>
- Lott, F., & Guez, L. (2013). A stochastic parameterization of the gravity waves due to convection and its impact on the equatorial stratosphere. *Journal of Geophysical Research: Atmospheres*, *118*, 8897–8909. <https://doi.org/10.1002/jgrd.50705>
- Lott, F., & Miller, M. J. (1997). A new subgrid-scale orographic drag parameterization: Its formulation and testing. *Quarterly Journal of the Royal Meteorological Society*, *123*(537), 101–127. <https://doi.org/10.1002/qj.49712353704>
- Manzini, E., Cagnazzo, C., Fogli, P. G., Bellucci, A., & Müller, W. A. (2012). Stratosphere-troposphere coupling at inter-decadal time scales: Implications for the North Atlantic ocean. *Geophysical Research Letters*, *39*, 105801. <https://doi.org/10.1029/2011GL050771>
- Manzini, E., & McFarlane, N. A. (1998). The effect of varying the source spectrum of a gravity wave parameterization in a middle atmosphere general circulation model. *Journal of Geophysical Research*, *103*(D24), 31,523–31,539. <https://doi.org/10.1029/98JD02274>
- Manzini, E., McFarlane, N. A., & McLandress, C. (1997). Impact of the Doppler spread parameterization on the simulation of the middle atmosphere circulation using the MA/ECHAM4 general circulation model. *Journal of Geophysical Research*, *102*(D22), 25,751–25,762. <https://doi.org/10.1029/97JD01096>
- McCormack, J., Eckermann, S. D., & Hogan, T. F. (2015). Generation of a quasi-biennial oscillation in an NWP model using a stochastic gravity wave drag parameterization. *Monthly Weather Review*, *143*(6), 2121–2147. <https://doi.org/10.1175/MWR-D-14-00208.1>
- McLandress, C. (1998). On the importance of gravity waves in the middle atmosphere and their parameterization in general circulation models. *Journal of Atmospheric and Solar-Terrestrial Physics*, *60*, 1357–1383. [https://doi.org/10.1016/S1364-6826\(98\)00061-3](https://doi.org/10.1016/S1364-6826(98)00061-3)
- McLandress, C., & Scinocca, J. F. (2005). The GCM response to current parameterizations of nonorographic gravity wave drag. *Journal of the Atmospheric Sciences*, *62*(7), 2394–2413. <https://doi.org/10.1175/JAS3483.1>
- Naujokat, B. (1986). An update of the observed quasi-biennial oscillation of the stratospheric winds over the tropics. *Journal of the Atmospheric Sciences*, *43*, 1873–1877. [https://doi.org/10.1175/1520-0469\(1986\)043<1873:AUOTOQ>2.0.CO;2](https://doi.org/10.1175/1520-0469(1986)043<1873:AUOTOQ>2.0.CO;2)
- Orr, A. (2009). The representation of non-orographic gravity waves in the IFS. Part II: A physically based spectral parameterization. ECMWF Tech. Mem.
- Orr, A., & Wedi, N. (2009). The representation of non-orographic gravity waves in the IFS. Part I: Assessment of the middle atmosphere climate with Rayleigh friction, ECMWF Tech. Mem.
- Palmer, T. N. (2001). A nonlinear dynamical perspective on model error: A proposal for non-local stochastic-dynamic parametrization in weather and climate prediction models. *Quarterly Journal of the Royal Meteorological Society*, *127*(572), 279–304. <https://doi.org/10.1002/qj.49712757202>
- Palmer, T. N. (2012). Towards the probabilistic Earth-system simulator: A vision for the future of climate and weather prediction. *Quarterly Journal of the Royal Meteorological Society*, *138*(665), 841–861. <https://doi.org/10.1002/qj.1923>
- Palmer, T. N., Shutts, G. J., & Swinbank, R. (1986). Alleviation of a systematic westerly bias in general circulation and numerical weather prediction models through an orographic gravity wave drag parameterization. *Quarterly Journal of the Royal Meteorological Society*, *112*(474), 1001–1039. <https://doi.org/10.1002/qj.49711247406>
- Pawson, S., Kodera, K., Hamilton, K., Shepherd, T. G., Beagley, S. R., Boville, B. A., et al. (2000). The GCM–reality intercomparison project for SPARC (GRIPS): Scientific issues and initial results. *Bulletin of the American Meteorological Society*, *81*(4), 781–796. [https://doi.org/10.1175/1520-0477\(2000\)081<0781:TGIPFS>2.3.CO;2](https://doi.org/10.1175/1520-0477(2000)081<0781:TGIPFS>2.3.CO;2)
- Piani, C., Norton, W. A., & Stainforth, D. A. (2004). Equatorial stratospheric response to variations in deterministic and stochastic gravity wave parameterizations. *Journal of Geophysical Research*, *109*, D14101. <https://doi.org/10.1029/2004JD004656>
- Polichtchouk, I., Shepherd, T. G., Hogan, R. J., & Bechtold, P. (2018). Sensitivity of the Brewer–Dobson circulation and polar vortex variability to parameterized nonorographic gravity wave drag in a high-resolution atmospheric model. *Journal of the Atmospheric Sciences*, *75*(5), 1525–1543. <https://doi.org/10.1175/JAS-D-17-0304.1>
- Roeckner, E., Bäuml, G., Bonaventura, L., Brokopf, R., Esch, M., Giorgetta, M., et al. (2003). The atmospheric general circulation model ECHAM5. Part I: Model description (MPI Report No. 349). Hamburg, Germany: Max Planck Institute for Meteorology.
- Schenzinger, V., Osprey, S., Gray, L., & Butchart, N. (2017). Defining metrics of the quasi-biennial oscillation in global climate models. *Geoscientific Model Development*, *10*(6), 2157–2168. <https://doi.org/10.5194/gmd-10-2157-2017>
- Schirber, S., Manzini, E., & Alexander, M. J. (2014). A convection-based gravity wave parameterization in a general circulation model: Implementation and improvements on the QBO. *Journal of Advances in Modeling Earth Systems*, *6*(1), 264–279. <https://doi.org/10.1002/2013MS000286>
- Schirber, S., Manzini, E., Krismer, T., & Giorgetta, M. A. (2015). The quasi-biennial oscillation in a warmer climate: Sensitivity to different gravity wave parameterizations. *Climate Dynamics*, *45*(3), 825–836. <https://doi.org/10.1007/s00382-014-2314-2>
- Taylor, K. E., Stouffer, R. J., & Meehl, G. A. (2012). An overview of CMIP5 and the experiment design. *Bulletin of the American Meteorological Society*, *93*(4), 485. <https://doi.org/10.1175/BAMS-D-11-00094.1>
- Williams, P. D., Haine, T. W. N., & Read, P. L. (2004). Stochastic resonance in a nonlinear model of a rotating, stratified shear flow, with a simple stochastic inertia-gravity wave parameterization. *Nonlinear Processes Geophysics*, *11*(1), 127–135. <https://doi.org/10.5194/npg-11-127-2004>